ChemComm

COMMUNICATION

Heteroleptic diradical Cr(III) complex with extended spin delocalization and large intramolecular magnetic exchange†

Received 00th January 2020,
Accepted ….

DOI: 10.1039/

rsc.li/chemcomm

Xiaozhou Ma,[a] Elizaveta A. Suturina,[b] Mathieu Rouzières,[a] Fabrice Wilhelm,[c] Andrei Rogalev,[c] Rodolphe Clérac,*[a] Pierre Dechambenoit*[a]

Successive chemical reductions of the heteroleptic complex [(tpy)Cr^{III}(tphz)]$^{3+}$ (tpy = terpyridine; tphz = tetrapyridophenazine) give rise to the mono- and di-radical redox isomers, [(tpy)Cr^{III}(tphz$^{\bullet-}$)]$^{2+}$ and [(tpy$^{\bullet-}$)Cr^{III}(tphz$^{\bullet-}$)]$^{+}$ respectively. As designed, the optimized overlap of the involved magnetic orbitals leads to extremely strong magnetic interactions between the *S* = 3/2 metal ion and *S* = 1/2 radical spins, affording well isolated S_T = 1 and S_T = 1/2 ground states at room temperature.

Extended spin delocalization in molecule-based materials is an attractive feature for spintronics[1] and for the design of permanent magnets.[2] This situation can be promoted using aromatic radicals, where unpaired electrons can be delocalized all over the π system. However, such a delocalization is usually much less marked when involving metal ions in coordination compounds, due to the symmetry and the relative orientations of the metal/ligand orbitals. This apparent problem can be bypassed by combining both magnetic metal ions and radical ligands in a single material and stabilizing strong magnetic exchange interactions between their spins,[3,4] which is strongly dependent on the overlap of their singly occupied orbitals.[4]

Recently, our group designed a series of dinuclear complexes based on Co(II) and Ni(II) metal ions and the redox-active tetrapyridophenazine (tphz)[5] as bridging ligand, and for which radical forms are accessible and particularly stable.[6,7] The magnetic interactions within the complexes can be tuned by successive reduction processes localized on the tphz ligand. Considering the particular tphz geometry and a *z* axis oriented along the N atoms of its pyridine groups, the d_{xy} orbital of a transition metal ion overlaps the best with the π-system of the aromatic bridging ligand, providing an excellent pathway for electron and spin delocalization. When this d_{xy} orbital is singly occupied like in the high-spin $3d^7$ Co(II) complex,[6] this configuration promotes dominating and massive antiferromagnetic Co-radical interactions (< -500 K; *-2J* formalism). Conversely, when d_{xy} is fully occupied for the $3d^8$ Ni(II) analogue, the orthogonality of the singly occupied d orbitals ($d_{x^2-y^2}$ and d_{z^2}) with the tphz$^{\bullet-}$ π-system leads to dominating and very strong ferromagnetic Ni-radical interactions (+214 K).[7] This comparison between Co(II) and Ni(II) complexes evidenced the pivotal role played by the d_{xy} orbital on the strength of the magnetic metal-radical coupling and its influence on the spin delocalization.[6,7]

Based on those conclusions, the $3d^3$ chromium(III) metal ion appears to be the best spin carrier candidate to promote the strongest metal-radical antiferromagnetic exchange. With Cr^{3+} in a pseudo-octahedral environment, all t_{2g} orbitals are singly occupied (Fig. S6, ESI†), which guarantees an optimized *π-d*

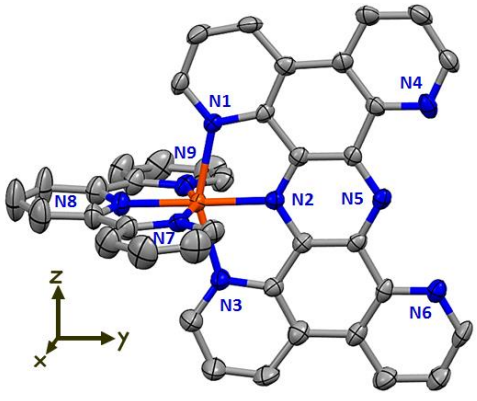

Fig. 1 Molecular structure of [Cr(tphz)(tpy)]$^{3+}$ in **1** at 120 K. Thermal ellipsoids are depicted at a 50 % probability level. Grey: carbon; orange: chromium; blue: nitrogen. Hydrogen atoms, solvent molecules and counter anions are omitted for clarity. Note that the depicted Cartesian axes are not the crystallographic axes, but the orientation chosen for the denomination of the *d* orbitals.

[a] Univ. Bordeaux, CNRS, Centre de Recherche Paul Pascal, UMR 5031, 33600 Pessac (France). E-mail: rodolphe.clerac@crpp.cnrs.fr; pierre.dechambenoit@crpp.cnrs.fr
[b] Department of Chemistry, University of Bath, Claverton Down, Bath BA2 7AY, UK
[c] ESRF-The European Synchrotron, 38043 Grenoble Cedex 9, France.

† Electronic Supplementary Information (ESI) available: experimental and synthetic methods, crystallographic data, UV/Vis/NIR and XAS spectroscopic spectra, cyclic voltammograms, Computational details, and additional magnetic data. CCDC 1954799-1954802. For ESI and crystallographic data in CIF or other electronic format see DOI: 10.1039/ x0xx00000x

overlap and thus an excellent electronic communication between the metal ions and the bridging ligand. Meanwhile, the empty e_g orbitals exclude the competing presence of ferromagnetic contributions to the exchange coupling as observed in the Co(II) and Ni(II) complexes due to the orthogonality of the singly occupied e_g orbitals and the bridging ligand SOMO.‡ As a consequences, only extremely large antiferromagnetic coupling is expected between Cr(III) and the tphz$^{\bullet-}$ radical spins.

To test this hypothesis and validate our synthetic strategy toward complexes with large intramolecular interactions, a novel series of Cr(III) complexes based on the redox-active tphz ligand is reported. The reaction of an equimolar mixture of Cr(tpy)$(CF_3SO_3)_3$[8] and tphz in CH_3CN leads to $[Cr(tphz)(tpy)](CF_3SO_3)_3 \bullet Et_2O$ (**1**), a new mononuclear chromium complex. Orange needle-shape crystals of **1** were isolated after slow diffusion of Et_2O vapors (ESI†). As confirmed by single crystal X-ray diffraction data at 120 K (Fig. 1, Table S1, ESI†), the Cr ion resides in an octahedral environment bonded to three nitrogen atoms from tphz and another three from tpy. The valence of the Cr metal ions is consistent with a +3 oxidation state according to bond valence sum calculation[9] and by comparison of the Cr-N bond lengths (Table 1) with similar complexes[10-12] and with the starting material $Cr^{III}(tpy)(CF_3SO_3)_3$ (Fig. S1, ESI†). In the crystal packing, the tricationic complexes are dimerized by π-π interactions between tphz ($d_{tphz\text{-}tphz}$ = 3.15 Å, Fig. S2, ESI†), and are separated by the triflate counter anions and diethylether lattice molecules.

The presence of a free coordination site on the tphz ligand in **1** prompted us to evaluate the possibility to coordinate another $[(tpy)Cr]^{3+}$ or $[(tpy)Co]^{2+}$ moiety on **1**. Unfortunately, this approach was unsuccessful. It seems that when the $[(tpy)Cr]^{3+}$ moiety is coordinated to one side of tphz, the small Cr^{III} radius together with the tphz rigidity give rise to a large N4-N6 distance (4.93 Å) at the free coordination site, which no longer fits another small metal ion like Cr^{III}. However, larger metal ions could fit, making this complex a potential switchable building-block for heterometallic architectures.[11]

Considering the redox-activity of both ligands[6,7] in the $[(tpy)Cr^{III}(tphz)]^{3+}$ cation, the possibility to isolate complexes based on chemically reduced ligands was explored. With one or two equivalents of cobaltocene, the corresponding redox isomers $[(tpy)Cr^{III}(tphz^{\bullet-})]^{2+}$ and $[(tpy^{\bullet-})Cr^{III}(tphz^{\bullet-})]^{+}$ were isolated in $[Cr^{III}(tphz^{\bullet-})(tpy)](CF_3SO_3)_2 \bullet CH_3CN$ (**1^{red}**, brown needle-shape crystals) and $[Cr^{III}(tphz^{\bullet-})(tpy^{\bullet-})]_2(CF_3SO_3)_2 \bullet 3CH_3CN \bullet 2Et_2O$ (**1^{redred}**, black plate-shape crystals) after slow diffusion of diethylether in their respective acetonitrile solution (ESI†). Both compounds crystallize in the triclinic *P*-1 space group (Table S1, ESI†) and differ by the number of counter anions per cationic unit. Within the three complexes, substantial differences are revealed when comparing the bond distances (Table 1). In particular, upon the first reduction, the significant decrease of the Cr-N2 bond length together with an elongation of the N2···N5 distances in the tphz pyrazine ring constitute important signatures of the tphz reduction into a radical form, tphz$^{\bullet-}$.[6,7] This conclusion is further supported by the absence of significant bond length changes within the tpy ligand, and by X-ray absorption spectroscopy (XAS) at the Cr K-edge of **1** and **1^{red}** (Fig. S3, ESI†) which evidences the same +3 oxidation state for the chromium site (see comments in the ESI†). Upon the second reduction, the bond distances remain similar for the tphz ligand, whereas noticeable changes are observed for the terpyridine. The increase of the average C-C and C-N bond lengths in the aromatic tpy rings and a shortening of the non-aromatic C-C bonds from *ca.* 1.47 to 1.45 Å (Table 1) are in perfect agreement with the observations made for the reduction of $Cr^{III}(tpy)_2^{3+}$ into $Cr^{III}(tpy^{\bullet-})_2^{+}$.[10] The presence of a tpy$^{\bullet-}$ radical is further supported by characteristic $\pi^* \rightarrow \pi^*$ absorption bands in the NIR region at 973 and 1130 nm, comparable with the spectroscopic signature observed for Li(tpy$^{\bullet-}$) (940 nm)[13] and Cr(tpy$^{\bullet-}$)$_2$(PF_6) (883 and 1120 nm)[10] (see Fig. S4, ESI†). As observed in the crystal packing of **1**, both reduced complexes are dimerized in **1^{red}** and **1^{redred}** by π-π interactions between tphz ligands ($d_{tphz\text{-}tphz}$ = 3.33 and 3.25 Å respectively; Fig. S2, ESI†).

The redox-activity of the complexes was also studied by cyclic voltammetry in acetonitrile. Remarkably, not less than six reversible reduction processes were detected for this mononuclear complex, at 0.11, -0.77, -1.21, -1.90, -2.11 and -2.36 V *vs.* Fc^+/Fc (Figure 2). Each redox process involves one

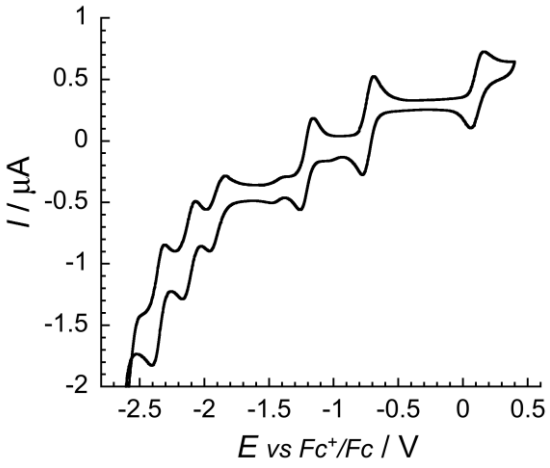

Fig. 2 Cyclic voltammogram for a solution of **1^{redred}** in CH_3CN at a 0.01 V/s scan rate, and 0.1 M (n-Bu_4N)PF_6 as supporting electrolyte. Further information can be found in the ESI† (Fig. S5).

Table 1 Selected bond distances (Å) at 120K.

	1	**1^{red}**	**1^{redred}**
Cr-N1	2.143(6)	2.119(6)	2.126(2)
Cr-N2	1.980(6)	1.900(6)	1.912(2)
Cr-N3	2.122(6)	2.108(6)	2.125(2)
Cr-N7	2.054(6)	2.065(6)	2.039(2)
Cr-N8	1.973(6)	1.998(6)	1.936(2)
Cr-N9	2.050(6)	2.065(6)	2.066(2)
N2···N5	2.772	2.851	2.850
C-C(pyz)[a,b]	1.403	1.397	1.393
C-N(pyz)[a,b]	1.342	1.358	1.362
$d_{arom}(C_{py}\text{-}C_{py})$ in tpy[b]	1.377	1.377	1.388
$d_{non\text{-}arom}(C_{py}\text{-}C'_{py})$ in tpy[b]	1.468	1.473	1.449
$d(C_{py}\text{-}N_{py})$ in tpy[b]	1.349	1.355	1.369

[a] pyz = pyrazine part of tphz; [b] average distance

electron, as confirmed by measuring the rest potential of solutions of **1**, **1**^{red} and **1**^{redred}, respectively at 0.3, -0.1 and -0.8 V *vs.* Fc^+/Fc, prior recording the cyclic voltammograms, which were found to be identical (Fig. S5, ESI†). As discussed previously, combined analyses of bond distances and X-ray absorption spectroscopy allows to unambiguously assign the two first reduction as being centered on the tphz and tpy ligands respectively, leading to $[(tpy)Cr^{III}(tphz^{\bullet-})]^{2+}$ and $[(tpy^{\bullet-})Cr^{III}(tphz^{\bullet-})]^{+}$ species (*vide supra*). These results should be placed in parallel with the rich electrochemistry of $[Cr(tpy)_2]^{3+}$ reported by Wieghardt *et al.*,[10] who demonstrated that the most accessible four successive reductions are exclusively centered on the tpy ligands. Similarly, one can reasonably assume in the present system that the third and fourth reductions are centered on tphz and tpy, respectively, affording $[(tpy^{\bullet-})Cr^{III}(tphz^{2-})]$ and $[(tpy^{2-})Cr^{III}(tphz^{2-})]^{-}$, while the two last reductions are the signature of a third reduction of both ligands at the most negative potentials. However, the use of stronger reducing agents, such as KC_8, didn't allow us to isolate other more reduced redox isomers so far.

To probe the strength of the magnetic exchange coupling in these Cr^{III} based complexes, and experimentally confirm the key influence of a suitable population of the magnetic $3d$ orbitals, dc magnetic measurements were performed on polycrystalline samples of the three compounds (ESI†). Above 100 K, the χT products shown in Figure 3 for the three redox isomers are constant at 1.91, 1.04 and 0.42 cm^3 K mol^{-1} for **1**, **1**^{red} and **1**^{redred} respectively, indicating Curie-like behaviors. While for **1**, the above χT value is expected for a magnetically isolated S = 3/2 Cr^{III} center (1.875 cm^3 K mol^{-1} for g = 2) and consistent with similar mononuclear complexes containing a Cr^{III} metal ion (g = 2.02),[14] the results obtained for **1**^{red} and **1**^{redred} are incompatible with a simple Curie constant sum of the involved Cr^{III} and radical spins (2.25 and 2.625 cm^3 K mol^{-1}, respectively). This apparent discrepancy is indeed the expected signature of the extremely large intramolecular magnetic interactions in **1**^{red} and **1**^{redred}, separating energetically the spin ground state, S_T, from the excited states, which are not thermally accessible at room temperature. As targeted by selecting the $3d^3$ electronic configuration of the Cr^{III} metal ion, these massive interactions lead to complexes behaving as magnetically isolated S_T macrospins.[15] The χT products above 100 K (1.04 and 0.42 cm^3 K mol^{-1}, Fig. 3) for **1**^{red} and **1**^{redred} correspond then to S_T = 1 and S_T = 1/2 ground states, respectively, as a consequence of huge antiferromagnetic $J_{Cr\text{-}tphz^{\bullet-}}$ and $J_{Cr\text{-}tpy^{\bullet-}}$ exchange couplings. Staying in the temperature domain below 300 K, for which the complexes are stable, the susceptibility measurements take place in the limit where $J_{Cr\text{-}tphz^{\bullet-}} >> k_BT$ and $J_{Cr\text{-}tpy^{\bullet-}} >> k_BT$, and thus these interactions cannot be experimentally determined. On the other hand, a rough estimation of these interactions (-2J formalism) can be obtained from DFT calculations on the basis of the crystal structures: $J_{Cr\text{-}tphz^{\bullet-}}/k_B$ = -1875 and -1760 K for **1**^{red} and **1**^{redred}, respectively; and $J_{Cr\text{-}tpy^{\bullet-}}/k_B$ = -1686 K for **1**^{redred} (cf. Table S2 and comments in Figs. S11, S12, ESI†). These interaction values place all excited states at more than 5000 K above their respective ground state, which is thus the only thermally populated state at room temperature. As expected

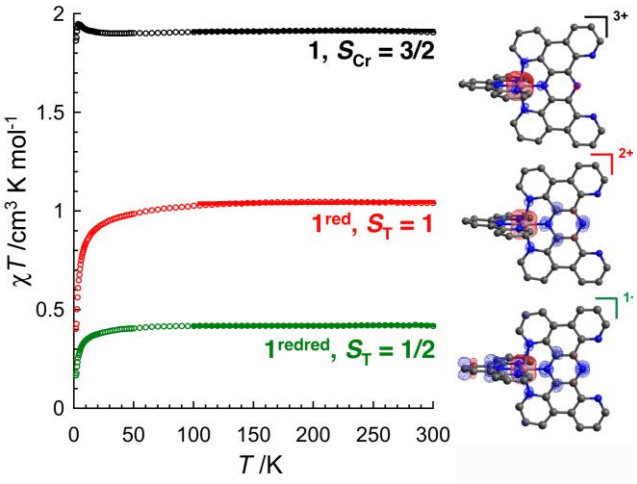

Fig. 3 Temperature dependence of the χT product for **1** (black), **1**^{red} (red) and **1**^{redred} (green) at 0.1 T between 1.85 and 40 K and at 1 T above 40 K (χ is defined as magnetic susceptibility equal to M/H per mole of complex). The solid lines represent the Curie limit at high temperature. Right side: corresponding spin density contour plots (0.005) of a broken-symmetry solution.

for the $3d^3$ configuration, the large $J_{Cr\text{-}tphz^{\bullet-}}$ coupling results from (i) an efficient overlap between the magnetic d_{xy} orbital of the Cr^{III} ion and the $tphz^{\bullet-}$ π system (Figs. S8 and S9, ESI†) as observed for a similar Co^{II}/tphz system,[6] and (ii) the absence of any antagonist ferromagnetic contribution arising from the population of orthogonal e_g orbitals (as seen in the Ni^{II}/tphz system).[7] Similarly, the large $J_{Cr\text{-}tpy^{\bullet-}}$ exchange originates from an equally good overlap of the π $tpy^{\bullet-}$ system with the d_{yz} Cr orbital (Fig. S9, ESI†).‡

Magnetic susceptibility measurements below 100 K (Fig. 3) reveals the presence of weak inter-complex magnetic interactions (ferromagnetic for **1** and antiferromagnetic for **1**^{red} and **1**^{redred}) likely induced by π-π stacking of the tphz ligand (Fig. S2, ESI†), and/or magnetic anisotropy caused by the distorted octahedral coordination sphere of the Cr(III) metal ions. These secondary effects are discussed in supporting information (Figs. S10-S12, ESI†). Additionally, for the three compounds, it is worth mentioning (i) the absence of out-of-phase ac susceptibility signal in our experimental window, and (ii) the lack of significant luminescence at room temperature in solid state.

In conclusion, and independently from those remarkably large antiferromagnetic exchange couplings, which experimentally confirm the key role of a suitable population of the magnetic orbitals, this Cr^{III}/tphz system is also a rare example of a complex containing two different ligands, which can be both reduced in a radical form. When doubly reduced, the spin density is fully delocalized on the three components of the complex as depicted in Figs. 3 and S9 (ESI†). The unpaired electrons of the t_{2g} shell form cubically shaped spin density at the Cr site, whereas the unpaired $tphz^{\bullet-}$ and $tpy^{\bullet-}$ electrons are delocalized on π-orbitals of the central pyrazine or pyridine groups, respectively. With the free coordination site of the tphz ligand, this kind of complex could also be used as a switchable magnetic and redox-active module for (supra)molecular architectures with higher dimensionalities or nuclearities.

This work was supported by the ANR (ANR-16-CE29-0001-01, Active-Magnet project), the University of Bordeaux, the Région Nouvelle Aquitaine, the CNRS, the MOLSPIN COST action CA15128 and the CSC for the PhD funding of XM. EAS thanks RSC for the Research Mobility grant and University of Bath HPC facility for computational resources. The authors thank the European Synchrotron Radiation Facility (ESRF, Grenoble, France) for the X-ray spectroscopy experiments and the GdR MCM-2 for fruitful discussions.

Conflicts of interest

There are no conflicts to declare.

Notes and references

‡ As the symmetry around the metal center is not strictly octahedral, the t_{2g} and e_g terms are not strictly accurate either, but they were used as an approximation to facilitate the discussion.

1 (a) J. M. Manriquez, G. T. Yee, R. S. McLean A. J. Epstein and J. S. Miller, *Science*, 1991, **252**, 1415; (b) M. Verdaguer, A. Bleuzen, V. Marvaud, J. Vaissermann, M. Seuleiman, C. Desplanches, A. Scuiller, C. Train, R. Garde, G. Gelly, C. Lomenech, I. Rosenman, P. Veillet, C. Cartier and F. Villain, *Coord. Chem. Rev.*, 1999, **190–192**, 1023; (c) E. Ruiz, A. Rodriguez-Fortea, S. Alvarez and M. Verdaguer, *Chem. Eur. J.*, 2005, **11**, 2135. (d) H. Phan, T. S. Herng, D. Wang, X. Li, W. Zeng, J. Ding, K. P. Loh, A. T. S. Wee and J. Wu, *Chem*, 2019, **5**, 1.

2 M. Gobbi, M. A. Novak and E. Del Barco, *J. Appl. Phys.*, 2019, **125**, 240401.

3 a) C. Coulon, H. Miyasaka and R. Clérac, *Struct. Bonding*, 2006, **122**, 163; b) W. Zhang, R. Ishikawa, B. Breedlove and M. Yamashita, *RSC Adv.*, 2013, **3**, 3772; c) C. Coulon, V. Pianet, M. Urdampilleta and R. Clérac, *Struct. Bonding*, 2015, **164**, 143.

4 O. Kahn, *Molecular magnetism*, VCH, Weinheim 1993.

5 (a) P. Bonhôte, A. Lecas and E. Amouyal, *Chem. Commun*., 1998, **8**, 885; (b) A. Gourdon and J.-P. Launay, *Inorg. Chem*., 1998, **37**, 5336.

6 X. Ma, E. A. Suturina, S. De, P. Négrier, M. Rouzières, R. Clérac and P. Dechambenoit, *Angew. Chem. Int. Ed.*, 2018, **57**, 7841.

7 X. Ma, E. A. Suturina, S. De, M. Rouzières, R. Clérac and P. Dechambenoit, *J. Am. Chem. Soc.*, 2019, **141**, 19, 7721.

8 The synthesis was made according the procedure reported in the following reference and the crystal structure is reported in Supplementary Information. E. C. Constable, C. E. Housecroft, M. Neuburger, J. Schönle and J. A. Zampese, *Dalton Trans.*, 2014, **43**, 7227.

9 I. Brown and D. Altermatt, *Acta Cryst. B*, 1985, **41**, 244.

10 C. C. Scarborough, K. M. Lancaster, S. DeBeer, T. Weyhermüller, S. Sproules and K. Wieghardt, *Inorg. Chem.*, 2012, **51**, 3718.

11. D. Zare, B. Doistau, H. Nozary, C. Besnard, L. Guénée, Y. Suffren, A.-L. Pelé, A. Hauser and C. Piguet, *Dalton Trans.*, 2017, **46**, 8992.

12. S. Otto, M. Grabolle, C. Förster, C. Kreitner, U. Resch-Genger and K. Heinze, *Angew. Chem. Int. Ed.*, 2015, **54**, 11572.

13. P. S. Braterman, J. L. Song and R. D. Peacock, *Inorg. Chem.*, 1992, **31**, 555.

14. C. C. Scarborough, S. Sproules, T. Weyhermüller, S. DeBeer and K. Wieghardt, *Inorg. Chem.*, 2011, **50**, 12446.

15. M. G.. Vinum, L. Voigt, C. Bell, D. Mihrin, R. W. Larsen, K. M. Clark and K. S. Pedersen, *Chem. Eur.J* .2020, **26**, 2143.

